Nuclear Materials and Energy 20 (2019) 100679

Contents lists available at ScienceDirect

Nuclear Materials and Energy

journal homepage: www.elsevier.com/locate/nme

Reaction processes of molecular activated recombination leading to detachment of divertor simulation plasma in GAMMA 10/PDX

A. Terakado[a,*], M. Sakamoto[a], N. Ezumi[a], K. Nojiri[a], T. Mikami[a], Y. Kinoshita[a], S. Togo[a], T. Iijima[a], K. Sawada[b], S. Kado[c], Y. Nakashima[a]

[a] Plasma Research Center, University of Tsukuba, 1-1-1 Tennodai, Tsukuba, Ibaraki 305-8577, Japan
[b] Faculty of Engineering, Shinshu University, 4-17- 1 Wakasato, Nagano 380-8553, Japan
[c] Institute of Advanced Energy, Kyoto University, Gokasho, Uji, Kyoto 611-0011, Japan

ARTICLE INFO

Keywords:
GAMMA 10/PDX
Divertor-simulation experiment
Plasma detachment
Molecular activated recombination
Molecular vibrational temperature
Population inversion

ABSTRACT

Reaction processes of molecular activated recombination (MAR) have been investigated using end loss plasma in GAMMA 10/PDX. A tungsten V-shaped target in a divertor simulation experimental module (D-module) is exposed to the end loss plasma. The additional hydrogen gas is supplied into the D-module, leading to the plasma detachment by MAR. The vibrational temperature (T_{vib}) of $H_2(X_1\Sigma_g^+)$ increased up to ~10,000 K with increasing the hydrogen gas pressure, and the H_a line intensity (I_{Ha}) continued to increase even though the electron density decreased after the electron density rollover. The increase in T_{vib} should be caused mainly by the increase in the number of vibrationally excited molecules which are produced by the molecular ion conversion process in MAR. The continuous increase in I_{Ha} is attributed to the dissociative attachment in MAR. When the hydrogen gas pressure was more than 12 Pa, Balmer emissions from highly excited atom suddenly increased and a population inversion with $n_{H(n=5)}$ larger than $n_{H\ (n=4)}$ was observed although T_{vib} became rather low (~2,000 K). The formation of population inversion and increase in highly excited Balmer line intensity are considered to be caused by the reaction of mutual neutralization between molecular ion and negative ion, since the cross section of $H(n = 5)$ production is the largest in the reaction. The negative ion should be produced by the resonant ionization process between H(2s), since the negative ion production by the dissociative attachment reaction cannot be expected due to low T_{vib}.

1. Introduction

Divertor detachment is the most promising solution to reduce heat load on a divertor plate. The plasma volumetric recombination by decreasing plasma temperature due to plasma-gas interaction (i.e. radiative cooling, inelastic collisions) leads to plasma detachment [1]. There are electron-ion recombination (EIR) and molecular activated recombination (MAR) as atomic molecular processes of volumetric recombination. The rate coefficient of MAR is much greater than that of EIR at relatively high electron temperature [2, 3]. Understanding reaction processes of MAR which leads to significant recombination at these elevated temperatures is important and the MAR phenomena leading to plasma detachment have been studied experimentally [4–6] and theoretically [7–9] for effective achievement of plasma detachment.

In GAMMA 10/PDX, a divertor simulation experimental module (D-module) has been installed in the west-end region, and divertor plasma phenomena such as production of detached plasma is being studied utilizing end-loss plasma as divertor simulation plasma [10]. The decrease of the electron temperature and rollover of the electron density (i.e. plasma detachment) have been observed by additional hydrogen gas supply to the divertor simulation plasma in D-module [11, 12]. The production mechanism of the detached plasma due to MAR related to triatomic hydrogen molecular ion (H_3^+) in the D-module has been suggested from the investigation of the atomic molecular processes based on the results of spectroscopic measurement [12]. It is suggested that the plasma detachment is promoted by the vibrationally excited molecules produced by MAR associated with H_3^+ in ref [12]. However, the population density of vibrationally excited hydrogen molecules in the D-module during detachment by MAR had not been evaluated. In this study, Fulcher-α band emission from hydrogen molecule was measured, and the vibrational temperature of the hydrogen molecule was estimated using corona model.

Besides, sudden increase in H_β, H_γ and H_δ emissions and population

* Corresponding author.
E-mail address: terakado_akihiro@prc.tsukuba.ac.jp (A. Terakado).

https://doi.org/10.1016/j.nme.2019.100679
Received 14 August 2018; Received in revised form 20 April 2019; Accepted 26 April 2019
Available online 07 May 2019

inversion with population density of H(n = 5) lager than that of H (n = 4) have been observed when the hydrogen gas pressure in the D-module becomes more than a certain value. In this study, atomic and molecular processes in the plasma detachment associated with MAR and the phenomena of population inversion are investigated from the observation of plasma parameters in the D-module such as electron temperature, electron density, Balmer line intensities and vibrational temperature of the hydrogen molecule.

2. Experimental setup

The GAMMA 10/PDX tandem mirror device consists of a central cell, anchor cells, plug/barrier cells and end regions [13]. The main plasma is produced and maintained by ion cyclotron range of frequency (ICRF) heating mainly at the central cell. The D-module is installed in the west end region of GAMMA 10/PDX. It consists of a rectangular box which has the dimension of 480 mm × 500 mm × 700 mm. A quartz window is attached on a side of D-module for measuring plasma emission. A V-shaped target covered with tungsten with the thickness of 0.2 mm is installed inside the D-module. The end-loss plasma of GAMMA 10/PDX flows from the plasma inlet at the in front panel of the D-module and the V-shaped target is exposed to the end-loss plasma. Langmuir probes are installed on the surface of the upper target plate, and the electron temperature (T_e) and electron density (n_e) are measured. Hydrogen Balmer line intensities are measured with low dispersion spectrometer (USB2000+, Ocean optics). Fulcher-a band spectrums and Balmer line emissions from hydrogen atom excited with principal quantum number of more than 5 are measured with high-dispersion spectrometer (SR500i, Ander). The relative sensitivities of the spectrometers were calibrated with a standard lump. The spatial resolution of each spectrometer is about 15 mm for USB2000+ and about 5 mm for SR500i. Measurement positions of the Langmuir probe and spectroscopes are shown in Fig. 1(a). The additional gas supply port is installed near the plasma inlet to supply hydrogen gas into the D-module. An ASDEX gauge, which can measure the neutral pressure in a magnetic field, is installed on the top of the D-module [14]. Fig. 2 shows the top view of the west end region together with the line of sight of spectrometers and a high-speed camera. The spatial distributions of H_a and H_b line intensities were measured with the high-speed camera with an interference filter in front of the lens of the camera.

3. Results

In the present experiments, the main plasma is produced and maintained by ICRF mainly in the central cell of GAMMA 10/PDX. Hydrogen gas was additionally supplied to the inside of the D-module from 300 ms before the plasma production until the end of plasma discharge. The amount of the additional hydrogen gas supply was changed shot by shot by changing the pressure in the reservoir tank (i.e. Plenum pressure) installed at the upstream of a piezoelectric valve. Fig. 3 shows time evolution of the neutral gas pressure (P_{H2}) in the D-module at each plenum pressure. The plasma was produced from 50 ms. The value of P_{H2} became constant before plasma discharge and increased after start of plasma discharge. The increase in pressure is attributed to suppress of out flow gas from the D-module due to plasma-gas interactions. It is noted that the ASDEX gauge installed in the D-module can be measured about 0.1 to 20 Pa [14], but it has not been calibrated at more than 20 Pa. Even so, in this study, ASDEX gauge would be able to measure at more than 20 Pa, since neutral pressure during plasma discharge is almost proportional to the plenum pressure.

Fig. 4 shows T_e, n_e and Balmer line intensities (I_{Ha}, I_{Hb}, I_{Hg} and I_{Hd}) in D-module as function of P_{H2}. We obtained several data from 100 ms to 220 ms in one plasma shot, and all of the data at each plenum pressure are plotted in Fig. 4. The electron temperature in front of the target plate decreased from about 25 eV to 1 eV or less with increasing P_{H2}. The electron density increased with increasing P_{H2} up to around

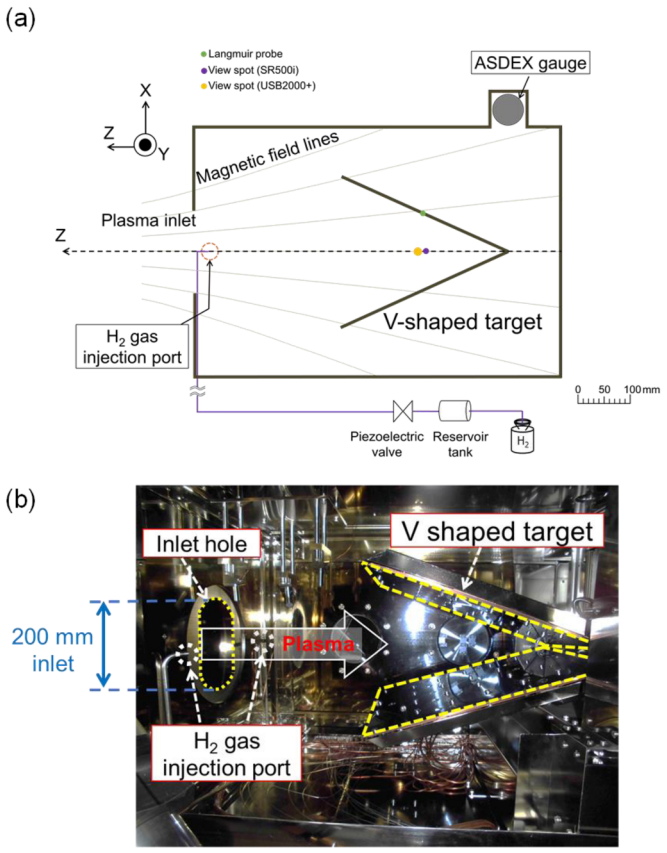

Fig. 1. (a) Schematic views and (b) photograph of the inside of the D-module.

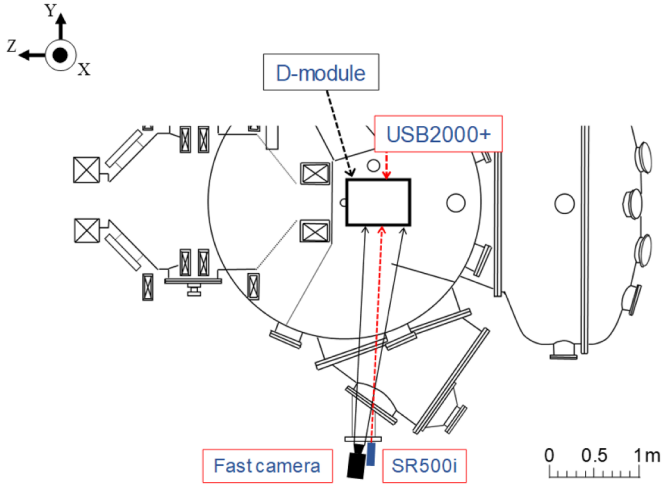

Fig. 2. (a) Top view of the west end region and line of sight of the spectrometers (USB2000+ and SR500i) and the fast camera and (b) measurement positions of Langmuir probe, USB2000+ and SR500i.

1.5 Pa and then it decreased, indicating a density rollover. In this study, T_e and n_e has not been obtained at the measurement position of spectroscopies shown in Fig. 1(a). According to the experimental operation almost same as this study in the D-module, the electron line-average density measured by the interferometer at the center of the plasma which is about one order of magnitude higher than n_e measured by the Langmuir probe on the target [15]. In addition, ref [15] reported that the pressure which showed rollover of line density was higher than the pressure which showed rollover of n_e measured by Langmuir probe on the target. Hence, it is suggested that T_e at the center of the plasma may be several eV higher than that of the measured Langmuir probe on the

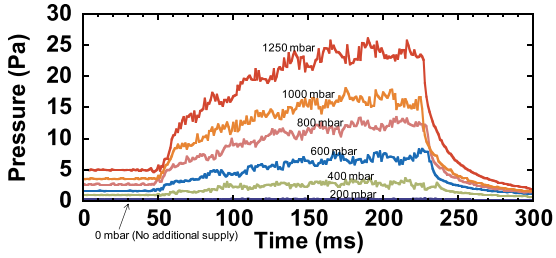

Fig. 3. Time evolution of the hydrogen gas pressure in the D-module, which is measured with the ASDEX gauge at each plenum pressure.

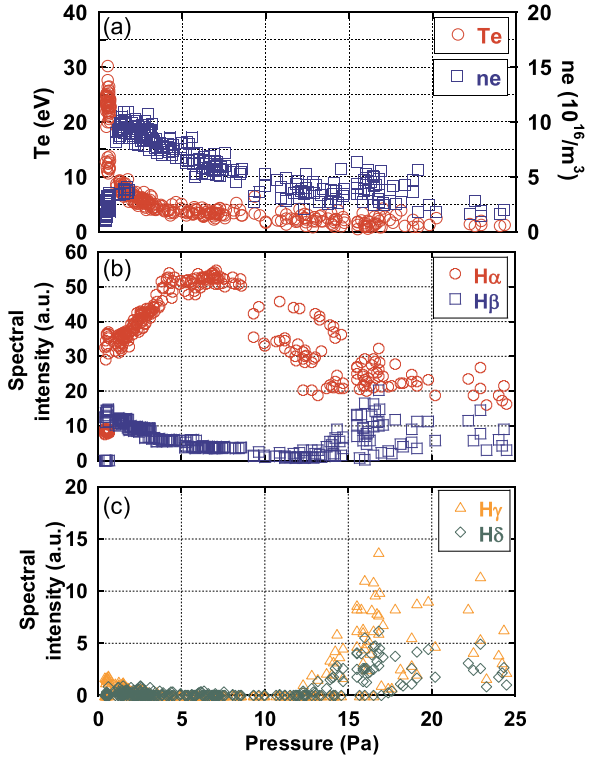

Fig. 4. (a) The electron temperature and electron density, (b) intensities of H_α and H_β emission, and (c) intensities of H_γ and H_δ emission measured by the spectroscopy (USB2000+) as a function of the hydrogen gas pressure.

target. The value of I_{Ha} increased with increasing P_{H2} up to about 8 Pa and then it decreased. The behaviors of I_{Hb}, I_{Hg} and I_{Hd} show the similar tendency to the electron density up to $P_{H2} \sim 12$ Pa. The value of I_{Hb}, I_{Hg} and I_{Hd} suddenly increased around $P_{H2} \sim 12$ Pa, but I_{Ha} hardly changed as shown in Fig. 4. The intensities of I_{Hb}, I_{Hg} and I_{Hd} saturated and decrease in higher pressure range (i.e. higher than around 20 Pa). It is noted that I_{Hb}, I_{Hg} and I_{Hd} increased from around 12 Pa which plenum pressure was 1000 mbar, whereas intensities of these increased from around 17 Pa which plenum pressure was 1250 mbar. The diamagnetism in the main plasma at the plasma shot with 1250 mbar of plenum pressure was decreased around 10% that of plasma shot with 1000 mbar of plenum pressure. It means that the main plasma and end-loss plasma was affected by the hydrogen gas which supplied into the D-module when plenum pressure was 1250 mbar, and that should be the reason for intensities increasing from 12 Pa and 17 Pa. The transition from lowly excited state of the hydrogen atom to highly excited state (i.e. the sudden increase in I_{Hb}, I_{Hg} and I_{Hd}) is hereinafter referred to as "High Excitation (HE) transition".

Fig. 5 shows the spatial distributions of the H_a and H_b line intensities measured with the high-speed camera before and after the HE transition. The spatial distribution of the H_b intensity changes drastically before and after the HE transition. A strong emission of the H_b was observed at the center of the plasma. The H_a line intensity decreases from the upstream toward the corner either before and after the HE transition.

Fig. 6 shows emission spectrum before and after the HE transition. It is noted that the data of Fig. 6 was obtained in an experiment campaign different from that of Fig. 3–5. The Balmer line emissions from highly excited atoms (H(n = 11)) were observed in the spectrum after the HE transition, although the Balmer emissions before the HE transition came from the excited atoms with n≦7. Fig. 7 shows the relative population density (n_n / g_n) obtained from the Balmer line intensities shown in Fig. 6. The value of n_n is evaluated from Balmer line intensity (I_{Ha}, I_{Hb}, I_{Hg} and I_{Hd}, etc.) divided by each Einstein coefficient (A_n). The value of $n_{H(n = 3)}$ hardly changes before and after the HE transition. Before the HE transition, the relative population density of more than n = 3 decreases with the excitation energy. On the other hand, a population inversion, which the value of $n_{H(n = 5)}$ was larger than $n_{H\ (n = 4)}$, was clearly observed after the HE transition.

Fig. 8(a) shows the Fulcher-α band spectrum before the HE transition at $P_{H2} \sim 8$ Pa. Fig. 8(b) shows the relative population density of $H_2(d^3\Pi_u^-)$ of 12 rovibrational states. The intensity of Fulcher-α band emission can be considered only with the inflow into the $d^3\Pi_u^-$ state from the electronic ground state ($X^1\Sigma_g^+$) due to electron impacts and the outflow from $d^3\Pi_u^-$ state to $a^3\Sigma_g^+$ state with spontaneous emission, because the collision frequency of electron impact with hydrogen molecules at the state of $d^3\Pi_u^-$ and $a^3\Sigma_g^+$ is rather small in low-density plasma (e.g. $n_e \leqq 10^{18}\ m^{-3}$) [16, 17]. Hence, the population distribution of vibrational level (i.e. vibrational temperature) in the electronic ground state can be associated with the intensity of Fulcher-a band emission by assuming the corona equilibrium for the electron impact excitation of $X^1\Sigma_g^+ \rightarrow d^3\Pi_u^-$ and spontaneous transition of $d^3\Pi_u^- \rightarrow a^3\Sigma_g^+$ [16]. The population density distribution of $H_2(d^3\Pi_u^-)$ agrees well with Boltzmann-Maxwellian distribution, and the vibrational temperature (T_{vib}) of $H_2(X^1\Sigma_g^+)$ can be estimated to be 10,000 K adapting the coronal model for states of $X^1\Sigma_g^+$, $d^3\Pi_u^-$ and $a^3\Sigma_g^+$ [16]. The value of T_{vib} increased from ~ 4000 K to ~10,000 K with increase in P_{H2} up to ~2 Pa and then decreased down to ~2000 K as shown in Fig. 9.

4. Discussion

4.1. Recombination processes of the detached plasma

In the previous study [12], it is suggested that the MAR process related to triatomic hydrogen molecules, which is the molecular ion conversion MAR (MIC-MAR) process shown in Table 1, would significantly contributes to the plasma detachment in GAMMA 10/PDX. The increase in I_{Ha} during the plasma detachment, which is shown in Fig. 4(b), should be caused mainly by the promotion of the dissociative attachment MAR (DA-MAR) process. Hence, the decrease in I_{Ha} from the upstream toward the corner as shown in Fig. 5(a) means that the occurrence of DA-MAR decreases from the upstream to the corner. The chain reaction in the DA-MAR process is promoted by the increase in the number of vibrationally excited molecules that are produced by the MIC-MAR process. We have estimated the population density of vibrationally excited molecules ($n_{H2(v)}$) from T_{vib} and P_{H2} (i.e. n_{H2}) assuming that the vibrational excitation level (v) of n_{H2} has Boltzmann-Maxwell distribution with T_{vib} and all of hydrogen molecules are at the electronic ground state ($X^1\Sigma_g^+$).

Fig. 10 shows $n_{H2(v)}$ as a function of v. The value of $n_{H2(v)}$ is significantly larger in the case of $P_{H2} \sim 11$ Pa than in the case of $P_{H2} \sim 1$ Pa, because T_{vib} is rather high (~ 10,000 K) when P_{H2} is ~ 11 Pa. It is revealed that the value of $n_{H2(v)}$ at $P_{H2} \sim 11$ Pa is about two order of magnitude larger than that at $P_{H2} \sim 1$ Pa, indicating that the vibrationally excited molecules are produced by the DR3 reaction.

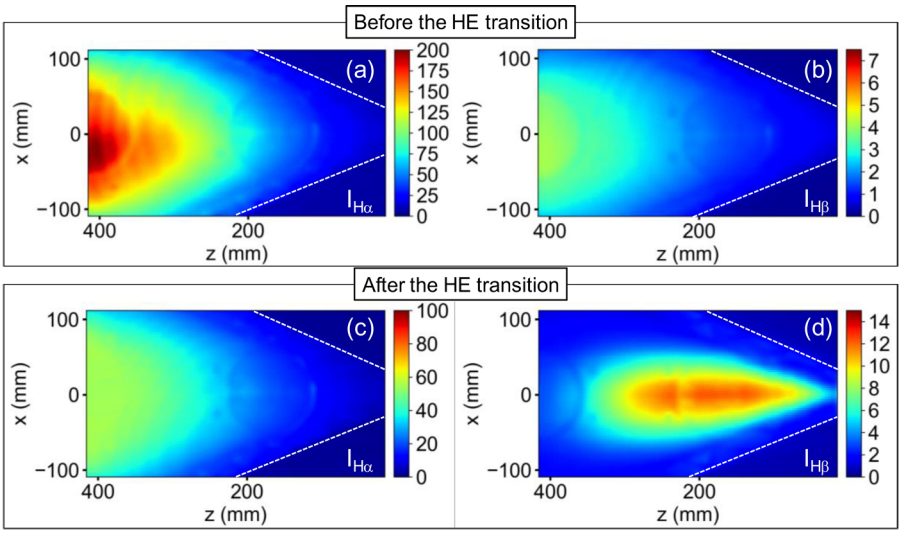

Fig. 5. Two-dimensional images of Balmer line intensities in front of the V-shaped target measured by the fast camera with an interference filter of which center wavelength is 656 nm or 486 nm and half maximum full-width is10 nm. (a) $I_{Hα}$ and (b) $I_{Hβ}$ before the HE transition. (c) $I_{Hα}$ and (d) $I_{Hβ}$ after the HE transition. White dash lines indicate the surface of V-shaped target.

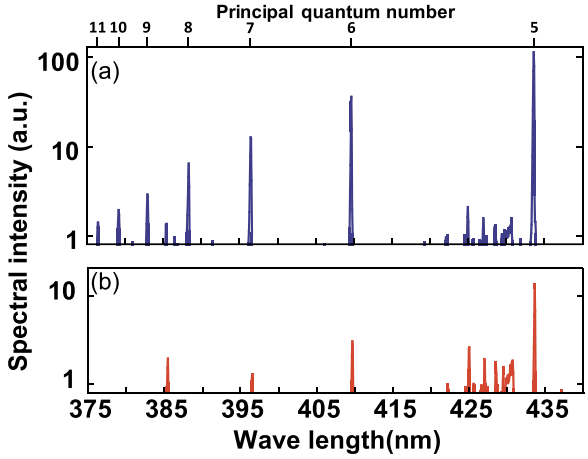

Fig. 6. The spectral intensities (a) after and (b) before the HE transition.

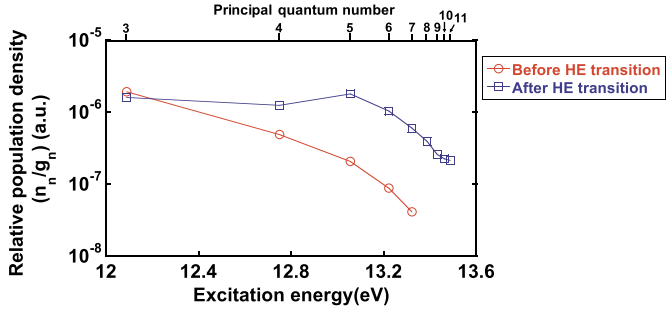

Fig. 7. Relative population density as a function of the excitation energy. The lines are a guide to the eye.

4.2. Mechanism of the population inversion

Sudden increase in I_{Hb}, I_{Hg} and I_{Hd} and population inversion are observed when P_{H2} is higher than 12 Pa as shown in Fig. 4. Furthermore, a strong emission of H_b was observed at the plasma center as shown in Fig. 5(d). The three-body recombination contributes to the formation of population inversion and production of highly excited atoms in the recombining plasma [18]. In this experiment, however, the three-body recombination cannot occur because n_e is rather low (i.e. $n_e \sim 3 \times 10^{16}$ /m^3) and $T_e \sim 1$ eV after the HE transition.

A possible candidate of the formation of the population inversion is

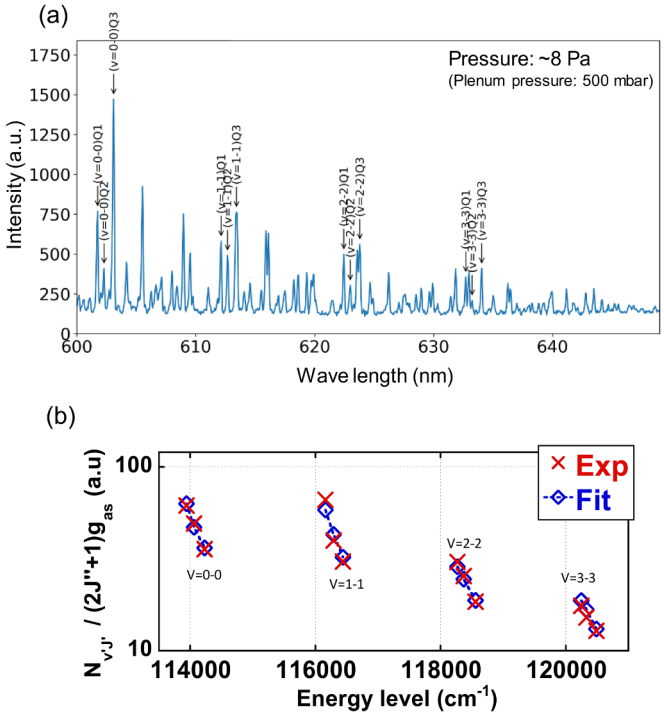

Fig. 8. (a) Fulcher-α band spectrum and (b) relative population densities of $d_3\Pi_u^-$ for various rovibrational states at the hydrogen gas pressure of 8 Pa.

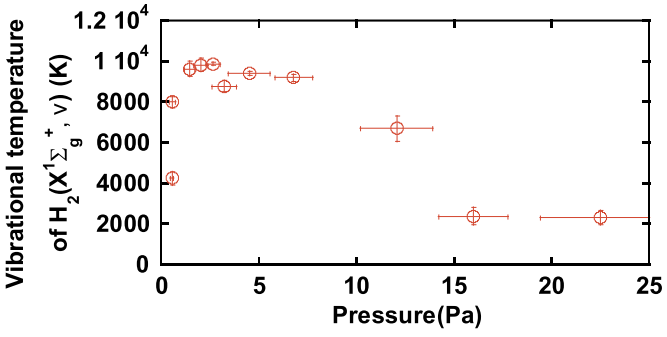

Fig. 9. Vibrational temperature as a function of the hydrogen gas pressure.

Table 1
Processes of molecular activated recombination in hydrogen plasma. The particle H_2^* refers to electrically excited molecular hydrogen. The notation (n) means principal quantum number and (v) means a vibrational quantum number.

Reaction name	Lable	Reaction
IC-MAR	CNV	$H_2(v) + H^+ \rightarrow H_2^+(v) + H$
	DR2	$H_2^+(v) + e \rightarrow H + H(n \geq 2)$
MIC-MAR	CNV	$H_2(v) + H^+ \rightarrow H_2^+(v) + H$
	CNV2	$H_2(v) + H_2^+(v) \rightarrow H_3^+(v) + H$
	DR3	$H_3^+(v) + e \rightarrow H_2(v) + H$
		$H_2^*(v) + H$
		$3H$
DA-MAR	DA	$H_2(v) + e \rightarrow H^- + H$
	NM	$H^- + H^+ \rightarrow H + H(n = 2, 3)$

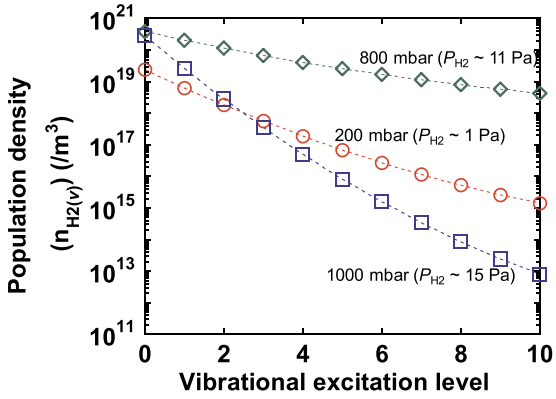

Fig. 10. Population density of hydrogen molecule $H_2(X_1\Sigma_g^+, v)$ at each plenum pressure. The lines are a guide to the eye.

the following reaction (hereinafter referred as MN2) [19, 20].

$$H_2^+ + H^- \rightarrow H_2 + H(n \geq 2). \quad (1)$$

Experimental results of cascaded arc discharge plasma in ref [21–23] showed population inversion similar to our experimental result. In the cross section of the MN2 reaction, H(n = 5) production is the largest [19]. Strong emission of H_b at the center of plasma as shown in Fig. 5(d) means that the MN2 reaction occurs mainly at the center of plasma. The intensities of I_{Hb}, I_{Hg} and I_{Hd} saturated and decreased in higher pressure range (i.e. higher than around 20 Pa) as shown in Fig. 4(b) and 4(c). In higher pressure range (i.e. higher than around 20 Pa), the CNV reaction would be suppressed (i.e. reduction of H_2^+ density) because the plasma density (i.e. density of hydrogen ion) decreased with the progress of plasma detachment. The saturated and decrease of I_{Hb}, I_{Hg} and I_{Hd} should be caused by the suppression of the MN2 reaction associated with decreasing density of H_2^+.

In our experiment, the number of H^- produced by the DA reaction should become rather low after the HE transition, since the population density of vibrationally excited molecules is low as shown in Fig. 10. As a process of H^- production leading to the MN2 reaction, a resonant ionization process [24–26] shown in the following equations seems to be a strong candidate:

$$H(2s) + H(2s) \rightarrow H^+ + H^-(2l2l'), \quad (2)$$

$$H^+ + H^-(2l2l') \rightarrow H_2^{**}, \quad (3)$$

$$H_2^{**} \rightarrow H^+ + H^-. \quad (4)$$

In the resonant ionization process, excited hydrogen atoms of H(2 s) react with each other to finally produce H^- by the chain reaction. It is expected that excited hydrogen atoms with n = 2 are still produced by the ion conversion MAR (IC-MAR) process after the HE transition, leading to the resonant ionization process. The MIC-MAR processes is considered to be suppressed since T_{vib} becomes rather low after the HE transition, leading to the suppression of DA-MAR process. On the other hand, the IC-MAR process does not depend largely on T_{vib}.

5. Summary

The reaction processes of MAR leading to plasma detachment have been investigated in the divertor simulation experiments on GAMMA 10/PDX. The electron temperature decreased from ~ 15 eV to ~ 1 eV with increasing P_{H2}. On the other hand, n_e increased with increasing P_{H2} up to ~1.5 Pa and then it decreased (i.e. so-called a density rollover), indicating the plasma detachment. The H_a line intensity continued to increase even though n_e decreased after the density rollover. The vibrational temperature of hydrogen molecule increased up to ~10,000 K with increasing P_{H2}. The population density of the vibrationally excited molecules also significantly increased with increasing P_{H2}, which is attributed to production of vibrationally excited molecules that are produced by the DR3 reaction of the MIC-MAR process. This increase in the vibrationally excited molecules caused the continuous increase in the H_a intensity after the density rollover through the DA-MAR process.

Sudden increase in I_{Hb}, I_{Hg} and I_{Hd} and population inversion (i.e. the HE transition) has been observed when P_{H2} is higher than 12 Pa. The population inversion seems to be caused by the MN2 reaction because the cross section of H(n = 5) production is the largest in the MN2 reaction. The negative ions for the MN2 reaction can be produced by resonant ionization process although the DA-MAR process, which produces the negative ions, becomes suppressed by decrease in T_{vib} after the HE transition. The excited hydrogen atoms with n = 2, which are used in the resonant ionization process, can be still produced by the IC-MAR process after the HE transition, since the cross section of the IC-MAR process does not depend largely on T_{vib}.

In this study, it was clarified that vibrationally excited molecules have an important role for the plasma detachment caused by MAR in the divertor simulation plasma of GAMMA 10/PDX. Besides, the present results suggested that the changes in the volumetric production process for H^- from DA to resonant ionization process and loss process for H^- from MN to MN2 by the increase in neutral pressure. These findings may help to research and development of negative ion source with the cesium-free operation [27] which volumetric negative ion production plays an important role, and low-temperature plasma sources [28]. Further studies such as direct measurement of the density of various ions (e.g. H^+, H_2^+, H_3^+, H^-) and estimation using CR-model are needed in order for quantitative evaluation for reaction processes.

Acknowledgment

This work is performed with the support of NIFS Collaborative Research Program (NIFS16KUGM119)

References

[1] S. Takamura, et al., Plasma Sources Sci. Technol. 11 (2002) A42–A48.
[2] A.Y. Pigarov, et al., Phys. Lett. A. 222 (1996) 251–257.
[3] N. Ezumi, et al., J. Nucl. Mater. 266–269 (1999) 337–342.
[4] J.L. Terry, et al., Phys. Plasmas. 5 (1998) 1759–1766.
[5] N. Ohno, et al., Phys. Rev. Lett. 81 (1998) 8181.
[6] S. Kado, et al., J. Nucl. Mater. 754 (2003) 131–316.
[7] R.K. Janev, et al., J. Nucl. Mater. 121 (1984) 10–16.
[8] D.E. Post, J. Nucl. Mater 220-222 (1995) 143–157.
[9] A.Y. Pigarov, et al., Phys. Scr. T96 (2002) 16.
[10] Y. Nakashima, et al., Nucl. Fusion. 116033 (2017) 1–8.
[11] K. Oki, et al., Fusion Sci. Technol. 68 (2015) 81–86.
[12] M. Sakamoto, et al., Nucl. Mater. Energy. 12 (2017) 1004–1009.
[13] M. Inutake, et al., Phys. Rev. Lett. 55 (1985) 939.
[14] K. Ichimura, et al., Rev. Sci. Instrum. 87 (2016) 11D424.
[15] J. Kohagura, et al., Rev. Sci. Instrum. 87 (2016) 11E127.
[16] B. Xiao, Plasma Phys. Control. Fusion 46 (2004) 653.

[17] E. Surrey, Plasma Phys. Control. Fusion 45 (2003) 1209.
[18] N. Ohno, et al., Nuclear Fusion 41 (2001) 1055.
[19] M.J.J. Eerden, et al., Phys. Rev. A. 51 (1995) 3362.
[20] C.L. Liu, et al., J. Phys. B At. Mol. Opt. Phys. 39 (2006) 1223–1229.
[21] O. Gabriel, et al., AIP Conf. Proc. 2009, pp. 22–30.
[22] W.E.N. Van Harskamp, et al., Phys. Rev. E - Stat. Nonlinear, Soft Matter Phys 83 (2011) 1–9.
[23] W.E.N. Van Harskamp, et al., Plasma Sources Sci. Technol (2012) 21.
[24] J. Komppula, et al., AIP Conf. Proc. 2013, pp. 66–73.
[25] J.S. Vogel, AIP Conf. Proc. 1655 (2015) 1–10 020015.
[26] J.S. Vogel, Rev. Sci. Instruments. 87 (2016) 1–3 2A503.
[27] J. Santoso, et al., Phys. Plasmas. 22 (2015) 093513.
[28] J. Ehlbeck, et al., J. Phys. D. Appl. Phys. 44 (2011) 013002.